

Atomic Energy of Canada Limited

CANDU-BLW EXPERIMENTS IN ZED-2

PART III:

BUCKLING AND LOSS OF COOLANT EXPERIMENTS

by

R. E. GREEN, R. E. KAY and C. W. COLPITTS

Chalk River, Ontario

May 1967

AECL-2691

CANDU-BLW EXPERIMENTS IN ZED-2

PART III: BUCKLING AND LOSS OF COOLANT
EXPERIMENTS

by

R.E. GREEN, R.E. KAY, C.W. COLPITTS*

A B S T R A C T

Experiments have been performed in simulated CANDU-BLW lattices in ZED-2 (square arrays of 28-rod UO_2 clusters at a spacing of 27.94 cm) to determine;

- (a) the material buckling of the lattice with H_2O or air as 'coolants',
- (b) the flux perturbation and reactivity effects of removing the H_2O coolant from 50% of the fuel assemblies in three geometric arrangements.

The buckling for the H_2O -cooled lattice was $1.166 \pm 0.018 \text{ m}^{-2}$, and for the air-cooled lattice $3.949 \pm 0.039 \text{ m}^{-2}$.

The loss of coolant experiments indicated a significantly smaller increase in reactivity when alternate fuel assemblies or alternate rows of fuel assemblies were voided than when one-half of the lattice about a diameter was voided.

*Summer student

AECL-2691

Chalk River, Ontario

May, 1967

TABLE OF CONTENTS

	<u>Page</u>
INTRODUCTION	1
FUEL AND LATTICE ARRANGEMENTS	2
EXPERIMENTS	9
1. Buckling Experiments	9
(a) General	9
(b) Critical Height Measurements	11
2. Coolant Loss Experiments	11
(a) Activity Distributions	11
(b) Cadmium Ratio Measurements	12
(c) Reactivity Measurements	12
RESULTS AND DISCUSSION	13
1. Buckling Experiments	13
(a) Cadmium Ratios	13
(b) Bucklings	13
(c) Extrapolation Lengths	17
2. Coolant Loss Experiments	18
(a) Activity Distributions	18
(b) Cadmium Ratios	23
(c) Reactivity Measurements	25
CONCLUSIONS	27
ACKNOWLEDGEMENTS	28
REFERENCES	29
APPENDIX A: Cadmium Ratio Measurements, Tables	
APPENDIX B: Buckling Measurements, Tables	

TABLES

CAPTION

	<u>Page</u>
1. Details of 28-Rod UO ₂ Fuel Assemblies	3
2. Summary of Buckling Measurements; 28 Rod UO ₂ Fuel, Air or H ₂ O Coolant	16
3. Summary of Extrapolation Lengths in 28 Rod UO ₂ , Air and H ₂ O Cooled Lattices	19
4. Cd Ratios and $r\sqrt{T/T_0}$ Values	23
5. Reactivity Effects of Coolant Loss	26

Appendix A

Cadmium Ratio Measurements; Various Lattices

Appendix B

Buckling Data; Various Lattices

FIGURES

CAPTION

	<u>Page</u>
1. Cross Section through 28 Rod Fuel Assembly	2
2. AQ Lattice in ZED-2; Buckling Measurements	4
3. BLW(AS) Lattice in ZED-2; Buckling Measurements	5
4. BLW(AV) Lattice in ZED-2; Buckling Measurements	5
5. AX Lattice in ZED-2; Buckling Measurements	6
6. 'Alternate Halves' Voided Lattice	7
7. 'Alternate Rows' Voided Lattice	8
8. 'Alternate Assembly' Voided Lattice	8
9. Indium Cadmium-Ratio Measurements in Air Cooled AQ Lattice	12
10. Indium Cadmium-Ratio Measurements in H ₂ O Cooled BLW(AS) Lattice	14
11. Indium Cadmium-Ratio Measurements in Air Cooled AX Lattice	14
12. North-South Radial Distributions in 'Alternate Halves' Voided Lattice	20
13. East-West Distributions in 'Alternate Halves Voided' Lattice	20
14. North-South Radial Distributions in 'Alternate Rows' Voided Lattice	21
15. East-West Distributions in 'Alternate Rows' Voided Lattice	21
16. North-South Radial Distributions in 'Alternate Assembly' Voided Lattice	22
17. East-West Distributions in 'Alternate Assembly' Voided Lattice	22
18. Cadmium Ratio Measurements in 'Alternate Assembly' Voided Lattice	24

INTRODUCTION

This is the third report of a series^(1,2) describing experiments to provide information on specific problems related to the proposed CANDU-BLW reactor to be built at Gentilly, Quebec.⁽³⁾

This report describes buckling measurements in the ZED-2 critical facility⁽⁴⁾ for 28-rod natural UO_2 fuel assemblies in heavy water moderator. These fuel assemblies, which were studied previously,⁽⁵⁾ simulated the fuel channels of the Gentilly power reactor. Measurements were made using air and H_2O as coolants to provide information on the variation of buckling with H_2O coolant density.

Also described are experiments to investigate the flux perturbation and reactivity effects of voiding one half of the 28-rod fuel assemblies, corresponding to a loss of coolant in one of the two primary coolant circuits. Three different geometrical arrangements of voided and filled channels were investigated to determine the effect of using different configurations for the coolant circuits.

FUEL AND LATTICE ARRANGEMENTS

Fig. 1 shows a cross sectional view of the 28-rod natural UO_2 fuel assembly, the details of which are given in Table 1. Each complete assembly contained five ~ 50 cm long fuel bundles.

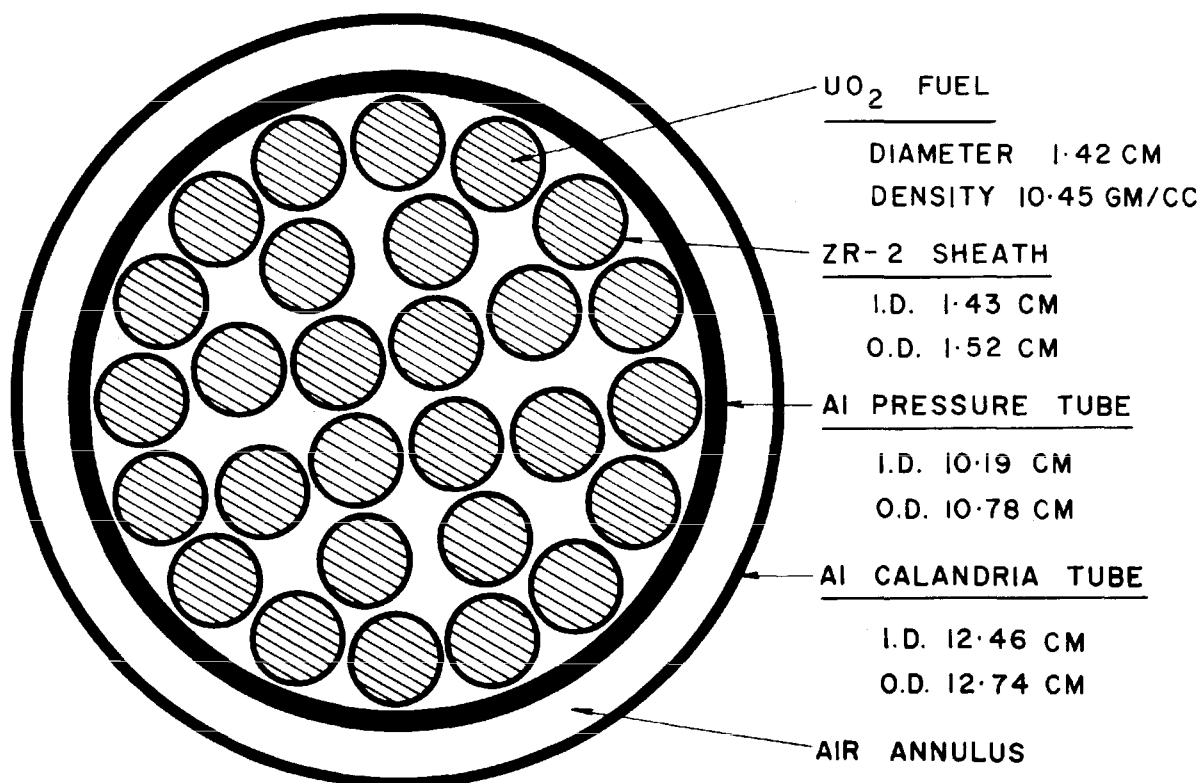


Fig. 1 Cross section through 28 rod fuel assembly

TABLE 1: DETAILS OF 28-ROD UO₂ FUEL ASSEMBLIES

Bundle:		
Layout		4 rods on 2.326 cm dia. circle 8 rods on 5.304 cm dia. circle 16 rods on 8.412 cm dia. circle
Overall length	cm	49.67
UO ₂ Fuel:		
Length per bundle	cm	47.73
Pellet diameter	cm	1.421
Density	g/cm ³	10.45
Fuel Sheath:		
Material		Zircaloy-2
Outside diameter	cm	1.522
Wall thickness	mm	0.454
Pressure Tube:		
Material		65S Aluminum
Outside diameter	cm	10.785
Wall thickness	mm	2.96
Calandria Tube:		
Material		50S Aluminum
Outside diameter	cm	12.738
Wall thickness	mm	1.39
Bundle End Plate:		
Material		65S Aluminum
Diameter	cm	10.16
Thickness	mm	3.18
Volume	cm ³	22.52
Bundle End Region: (a)		
Gap between UO ₂	cm	1.94
Volume of Zircaloy-2	cm ³	19.86
Volume of 65S Al	cm ³	45.05
Volume of air	cm ³	9.37
Volume of coolant	cm ³	84.05

(a) The bundle end region is defined as the region inside the pressure tube lying between the ends of the UO₂ fuel in adjacent bundles.

For the first air-cooled buckling experiment, the core arrangement consisted of fifty-three fuel assemblies arranged in a square lattice with a pitch of 27.94 cm as shown in Fig. 2.

Buckling experiments with H₂O coolant were performed for two different lattice arrangements as shown in Fig. 3 and 4. Fig. 3 shows the rod-centred lattice which contained, in addition to 53 of the 28-rod fuel assemblies, a "buffer region" of 20 air-cooled 7-rod UO₂ assemblies⁽⁶⁾ and a "driver region" of 120 ZEEP rods⁽⁷⁾ surrounding the central region. The open-centre lattice (shown in Fig. 4) contained 52 of the 28-rod UO₂ assemblies, 24 air-cooled 7-rod UO₂ assemblies and 112 ZEEP rods. The extra fuel assemblies were required to produce criticality with a moderator height less than the fuel height.

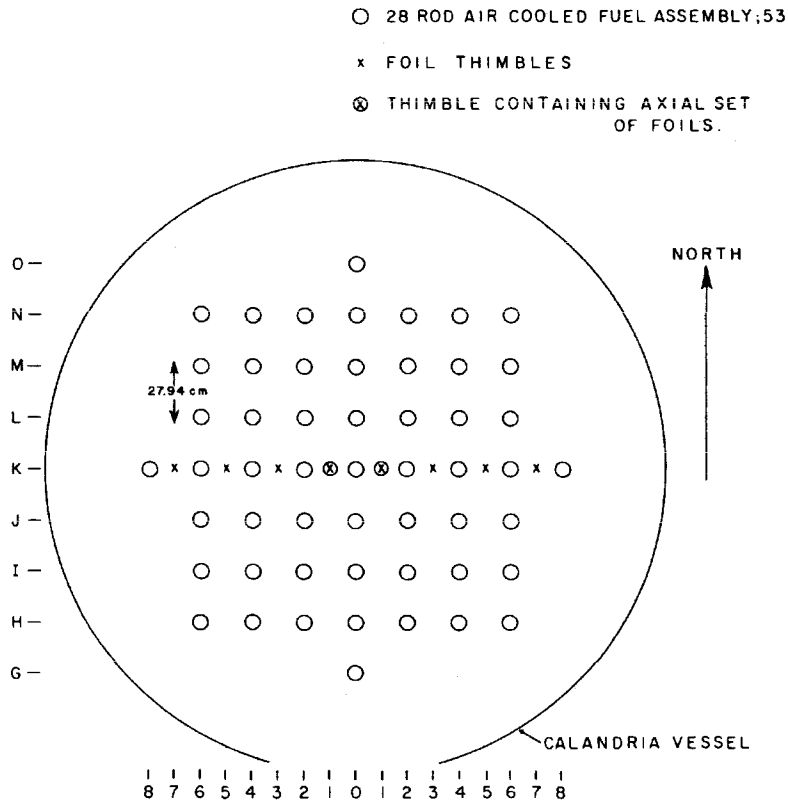


FIG. 2 : AQ LATTICE IN ZED - 2 ;
 BUCKLING MEASUREMENTS

- 28 ROD H₂O COOLED FUEL ASSEMBLY; 53
- 7 ROD FUEL ASSEMBLY; 20
- ZEEP FUEL ROD; 120
- x FOIL THIMBLES
- ⊗ THIMBLE CONTAINING AXIAL SET OF FOILS.

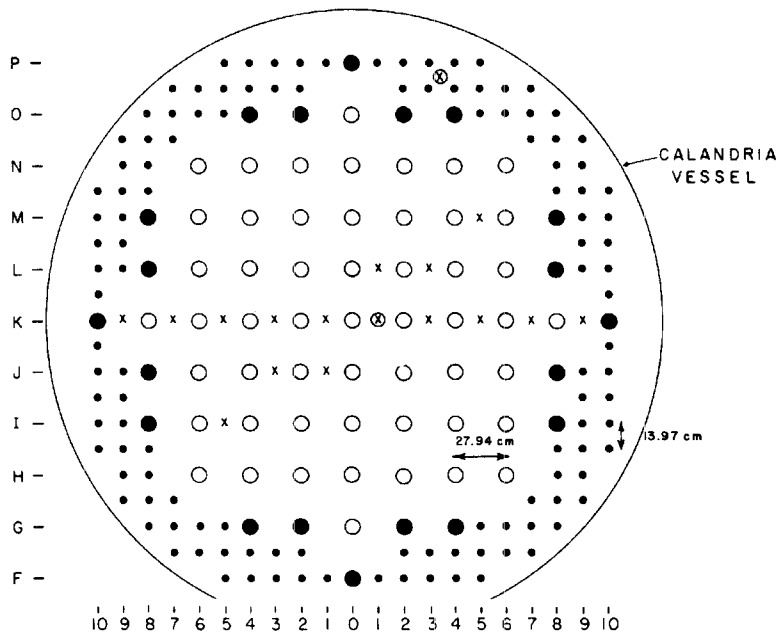


FIG. 3 : BLW (AS) LATTICE IN ZED-2;
BUCKLING MEASUREMENTS

- 28 ROD H₂O COOLED FUEL ASSEMBLY
- 7 ROD FUEL ASSEMBLY
- ZEEP FUEL ROD
- x FOIL THIMBLES
- ⊗ THIMBLE CONTAINING AXIAL SET OF FOILS

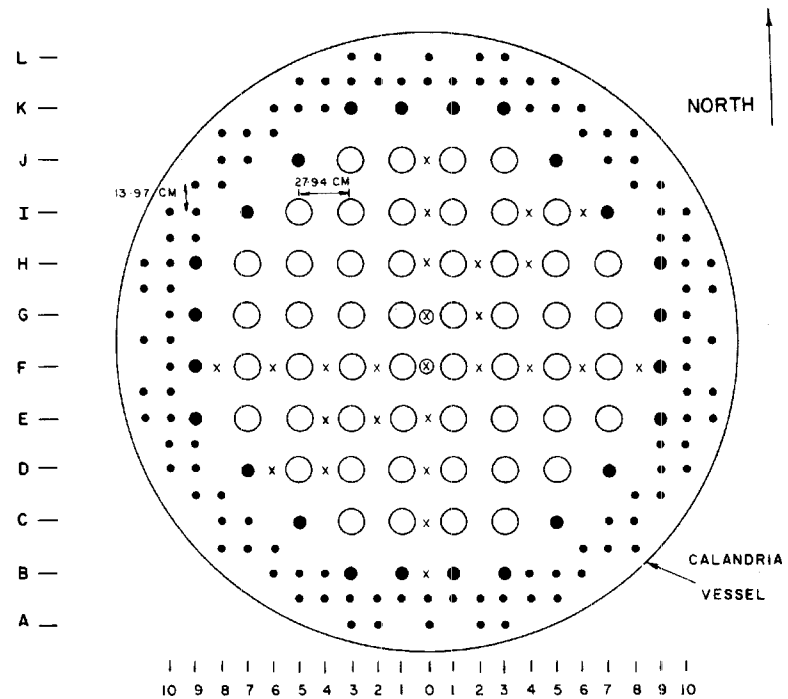


FIG. 4 : BLW (AV) LATTICE IN ZED-2;
BUCKLING MEASUREMENTS

The second air-cooled buckling experiment was performed using the lattice of Fig. 5. This lattice is geometrically identical with the BLW (AV) lattice of Fig. 4 but all the 28-rod fuel assemblies are air-cooled.

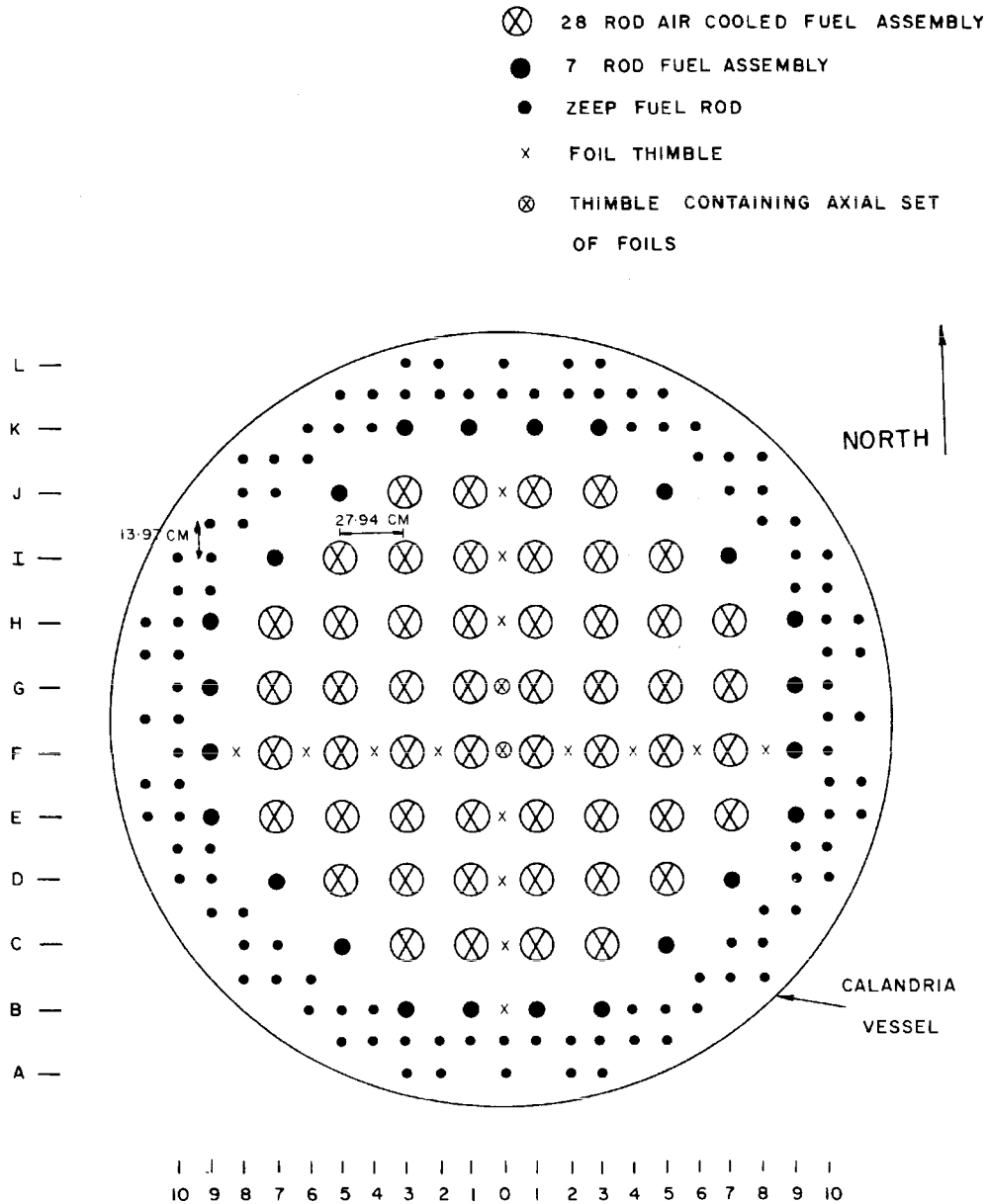


FIG. 5: AX LATTICE IN ZED-2 ;
BUCKLING MEASUREMENTS

The three geometrical configurations investigated in the coolant loss experiments are illustrated in Fig. 6 to 8. They were arranged as follows;

- (a) half of the lattice about a North-South diameter voided, designated 'alternate halves' (Fig. 6),
- (b) alternate rows of fuel assemblies voided (Fig. 7), and
- (c) alternate fuel assemblies voided (Fig. 8).

- 28 ROD FUEL ASSEMBLY
- 7 ROD FUEL ASSEMBLY
- ZEEP FUEL ROD
- ⊗ VOIDED 28 ROD ASSEMBLY
- x THIMBLE

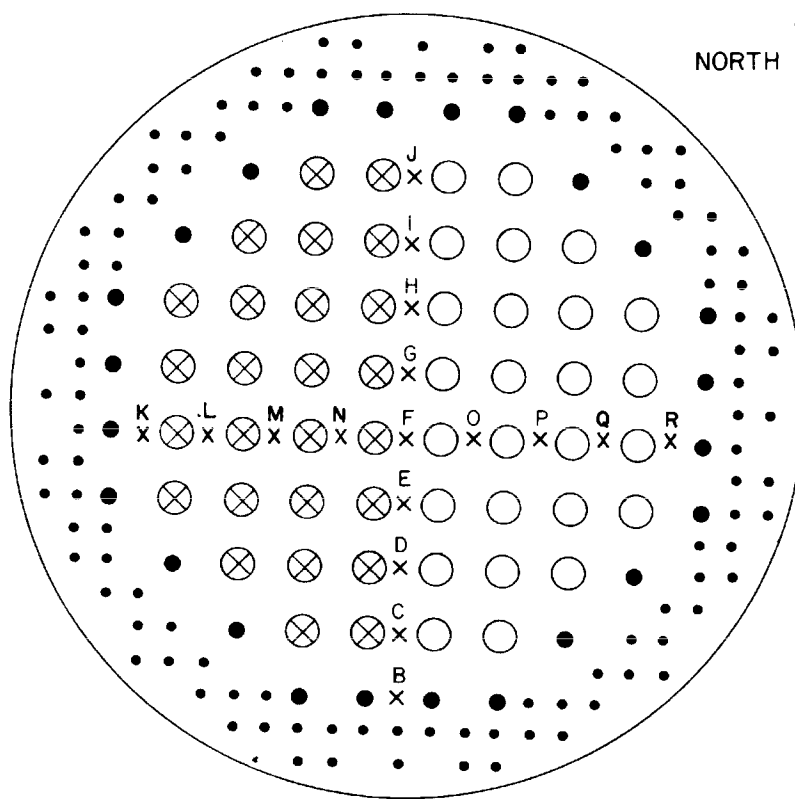


FIG. 6: 'ALTERNATE HALVES' VOIDED LATTICE

- 28 ROD FUEL ASSEMBLY
- 7 ROD FUEL ASSEMBLY
- ZEEP FUEL ROD
- ⊗ VOIDED 28 ROD ASSEMBLY
- x THIMBLE

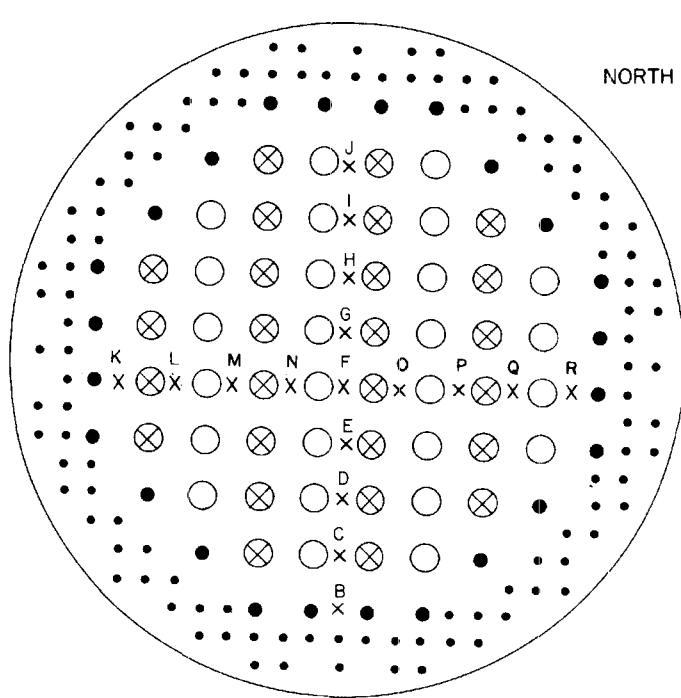


FIG. 7: 'ALTERNATE ROWS' VOIDED LATTICE

- 28 ROD FUEL ASSEMBLY
- 7 ROD FUEL ASSEMBLY
- ZEEP FUEL ROD
- ⊗ VOIDED 28 ROD ASSEMBLY
- x THIMBLE

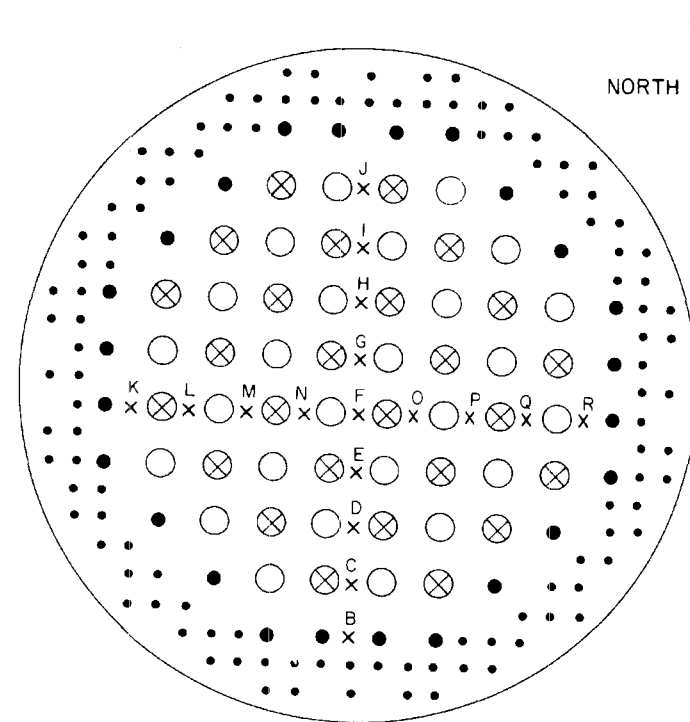


FIG. 8: 'ALTERNATE ASSEMBLY' VOIDED LATTICE

EXPERIMENTS

1. Buckling Experiments

(a) General

The material buckling was determined from foil activation measurements made at positions mid-way between adjacent fuel assemblies. Mn-10% Ni foils, 1.13 cm in diameter, weighing about 85 mg were used as neutron detectors. These were fixed to 25 x 20 x 0.5 mm aluminum backing plates which were joined by lengths of 0.076 cm diameter Zircaloy wire. The wire-foil system was supported in an air-filled aluminum thimble of cruciform cross-section. (5)

Fig. 2 to 5 show the locations of the measuring thimbles in the various lattices. In each case the thimbles contained two or three horizontal sets of foils located near the vertical flux maximum, and two thimbles contained detectors placed at 10 cm intervals over the entire moderator height (see Fig. 2, 3 and 4).

After irradiation the induced 2.58 hour ^{56}Mn activity was measured with an automatic counting system containing a TQQB electroscopes and sample changer. The ^{56}Mn activities, corrected for exponential decay, detector sensitivity, background and electroscopes drift essentially give the neutron density distribution throughout the lattice.

From homogeneous one-group diffusion theory, the fundamental neutron density distributions for a bare, critical cylindrical reactor of finite length with the origin located a distance z_0 from the flux maximum are;

$$\phi(z) = \phi(z_0) \cos \alpha (z-z_0) \quad (1)$$

for the axial distribution and

$$\phi(r) = \phi(o) J_0(\lambda r) \quad (2)$$

for the radial distribution,

where $\alpha^2 =$ axial buckling

$\lambda^2 =$ radial buckling

and the total buckling is given by,

$$B^2 = \alpha^2 + \lambda^2 \quad (3)$$

The above theory also applies to a bare, heterogenous reactor if the neutron density is measured at identical positions in each lattice cell. It is also usually assumed to be applicable to a reflected or 'driven' lattice for a region $\geq 1\frac{1}{2}$ neutron migration lengths inside the central core boundaries.

In the case where the central core is driven so that there is a net radial flow of neutrons inward, the radial neutron density distribution is given by

$$\phi(r) = \phi(o) I_0(\nu r) \quad (4)$$

and the buckling is then

$$B^2 = \alpha^2 - \nu^2 \quad (5)$$

This situation arises here for the H₂O-cooled lattices since $B^2 < \alpha^2$ for these lattices.

The region in which one-group theory is applicable is usually determined by measuring the Cd ratio for a given neutron detector throughout the lattice; where the Cd ratio is constant, one-group theory is assumed to be valid. For the lattices

studied here, Cd ratios were measured at various radial positions near the vertical flux maximum using 1.13 cm diameter, 0.013 cm thick, 1% In-Al foils and 0.076 cm thick Cd covers. From the results the radial region where one-group theory is valid was determined. The axial region was taken to be that found in previous experiments in similar lattices.⁽⁵⁾

(b) Critical Height Measurements

An accurate determination of the critical moderator level was required for determination of foil loading corrections and derivation of axial extrapolation lengths. Measurements of the moderator height were made with the accurate height indicator described in AECL-1505.⁽⁶⁾ With this instrument, changes in moderator level can be determined to ± 0.005 cm; absolute levels are known to ± 0.2 cm.

2. Coolant Loss Experiments

In the three partially voided lattices foil activity distributions and Cd ratios for In were measured for various directions throughout the lattice.

(a) Activity Distributions

Foil activity distributions were determined using 1.13 cm dia., 0.025 cm thick Cu foils mounted in the Al thimbles and suspended at cell edge locations across the lattice. The locations of these thimbles are shown in Fig. 6 to 8. Thimbles B to J and K to R held foils at elevations of 75 cm and 105 cm (relative to the floor of the calandria vessel) in all experiments. In addition thimbles M and P or F and G held a complete set of foils at 10 cm intervals from 15 cm to 175 cm elevation.

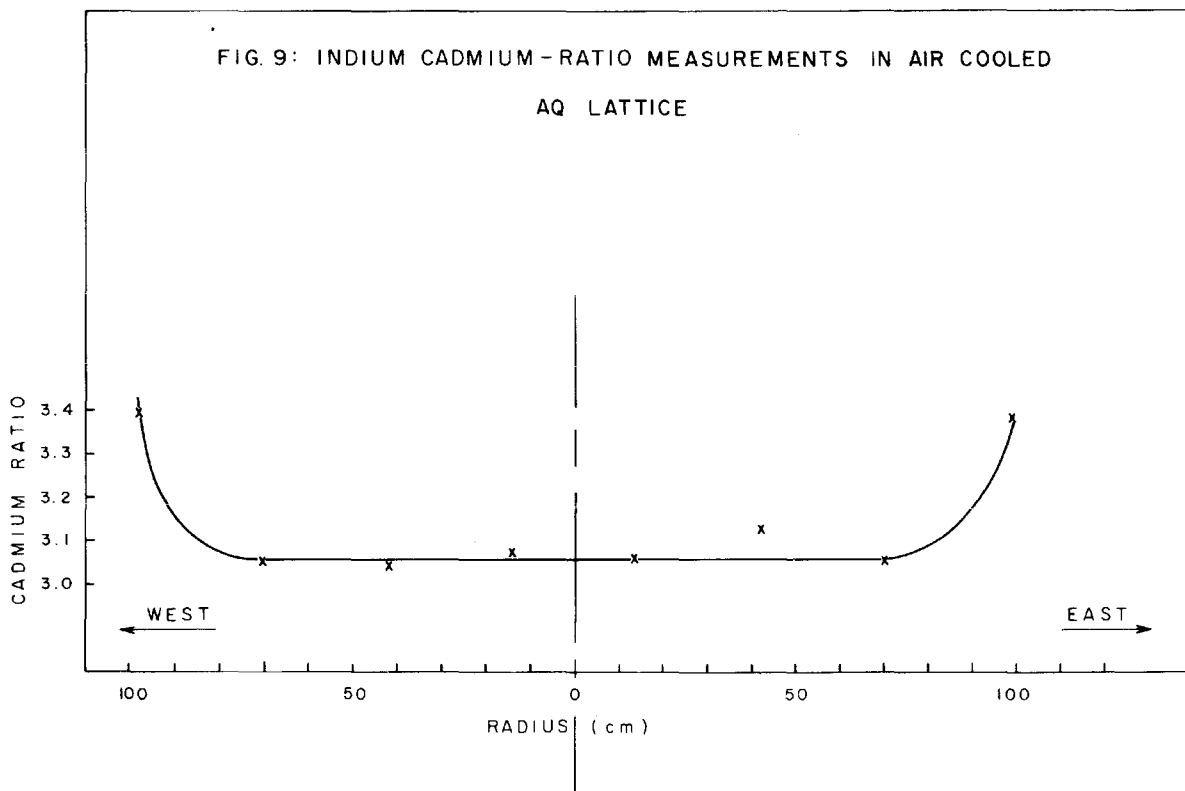
(b) Cadmium Ratio Measurements

Cadmium ratio measurements were made in the 'alternate fuel assembly' lattice of Fig. 8 using 0.013 cm thick, 1.13 cm dia., 1% In-Al foils and 0.076 cm thick Cd and Al boxes placed at elevations of 75 cm and 105 cm in thimbles B to R.

(c) Reactivity Measurements

In order to determine the reactivity effect of voiding various fuel channels, pile critical heavy water heights were determined for the following lattice configurations:

- (a) 'Alternate halves' voided
- (b) 'Alternate rows' voided
- (c) 'Alternate assemblies' voided
- (d) All 28-rod fuel assemblies voided
(i.e. lattices AX and AQ).



RESULTS AND DISCUSSION

1. Buckling Experiments

(a) Cadmium Ratios

The results of the Cd ratio measurements are listed in Tables A1 to A4 of Appendix A. These data are shown graphically in Fig. 9-11. From these results the radial region used in fitting the Mn-Ni activation data was taken as,

$$r < 90 \text{ cm}$$

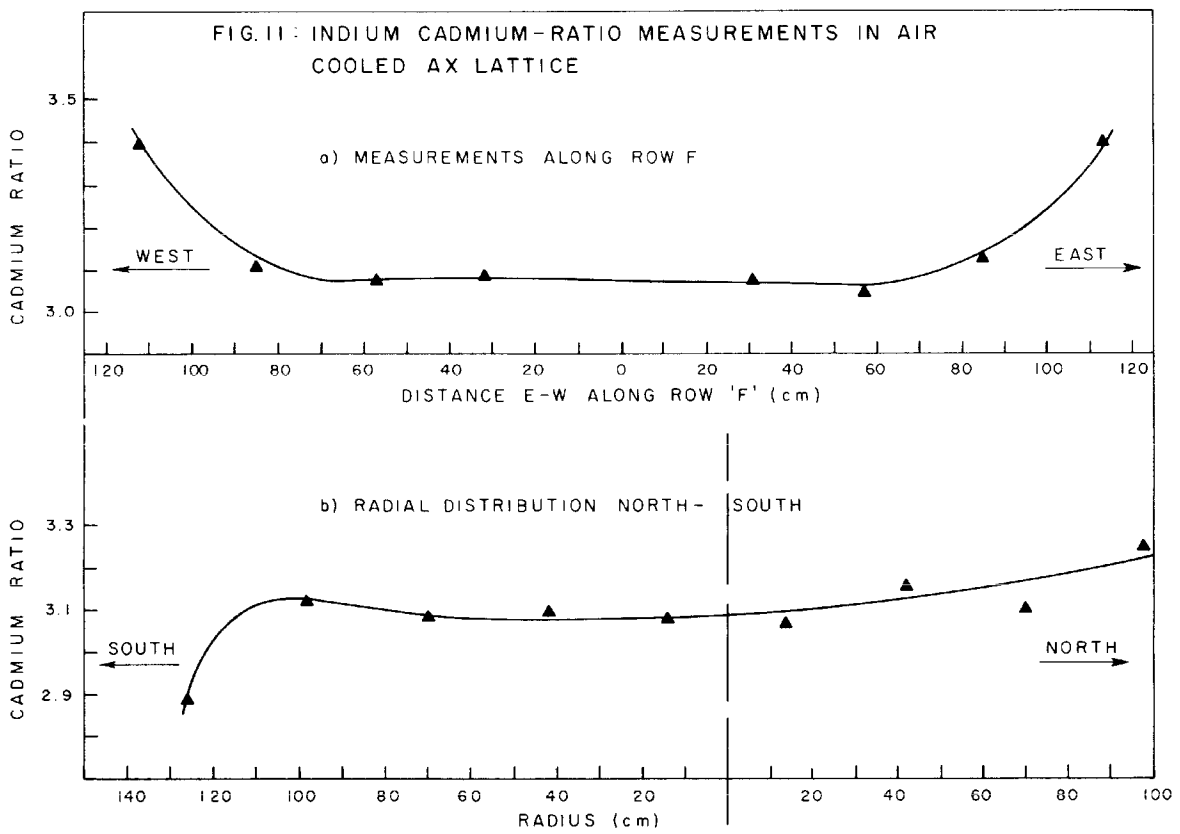
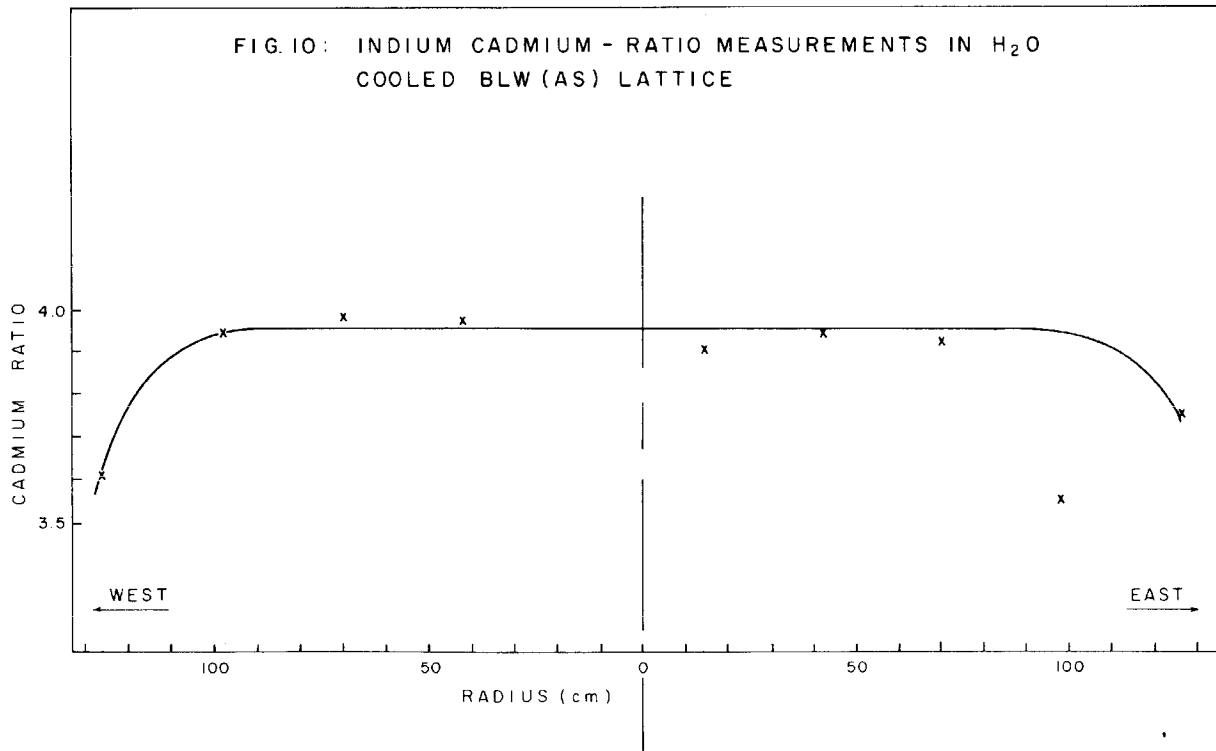
The axial region was determined from previous experiments⁽⁵⁾ to be

$$45 < z < H_{D_2O} - 25 \text{ cm}$$

with a maximum value of $z = 235$ cm (since the top of the fuel is at an elevation of 263 cm), where H_{D_2O} is the D_2O moderator critical level.

(b) Bucklings

The results of the Mn-Ni foil activation measurements are given in Tables B1 to B5 of Appendix B. Foil elevations and critical moderator heights are both measured with respect to the ZED-2 calandria floor. The activation data were fitted by the method of least-squares to the appropriate functions of equations (1), (2), and (4). The bracketed values in Tables B1 to B5 were not in the region of constant cadmium-ratio and thus were not included in the fitting. The results of the fitting are given at the bottoms of the tables. When more than one fit was possible the final value of z_0 , α , λ , or ν was taken as the mean of the several values. For the H_2O -cooled



lattices more radial thimbles were used and in the fitting the East and Northeast (West and Southwest) data were combined.

The error quoted for each α , λ , ν and z_0 value is

- (1) the error obtained from the "goodness-of-fit" of the data to the assumed distribution functions, or
- (2) the standard deviation in the mean of the several values obtained for each parameter,

whichever is the larger.

The buckling results are summarized in Table 2. Corrections for foil and thimble loading effects and small temperature and D_2O purity variations during the period of measurements were applied to give a consistent set of buckling values.

Corrections for the loading effect were obtained from measurements of the critical height with and without thimbles and foils in the core, viz.,

$$\alpha = \frac{\pi}{\pi/\alpha_{\text{fit}} - \Delta H} \quad (6)$$

where α_{fit} is the value derived from the fit, and ΔH is the difference in critical height with and without foils and thimbles. The variation in the radial buckling with loading was assumed to be negligible.

The heavy water purity decreased from 99.72 to 99.66 atom % D_2O during the experiments and the moderator temperature varied from 21.8°C to 22.6°C.

The final experimental buckling values given in Table 2 have been corrected to a moderator temperature of 25°C and purity of 99.70 atom % D_2O using purity and temperature coefficients of buckling predicted by the lattice recipe code P000F. (8)

TABLE 2: SUMMARY OF BUCKLING MEASUREMENTS; 28 ROD UO₂
 FUEL, AIR OR H₂O COOLANT

Lattice	Coolant	Table No.	* α^2 m ⁻²	λ^2 or [ν^2] m ⁻²	ΔB^2_T m ⁻²	ΔB^2_p m ⁻²	B ² (25°C; 99.70 at % D ₂ O) m ⁻²	B ² average m ⁻²	LATREP m ⁻²	POOF m ⁻²
AQ	AIR	B-1	1.943±0.015	2.063±0.040	-0.018	-0.011	3.977±0.042	3.949±0.039	3.610	3.879
AX	AIR	B-5	3.015±0.029	0.865±0.032	-0.003	+0.043	3.920±0.043			
AS	H ₂ O	B-2	1.4114±0.0082	[0.238±0.014]	-0.003	-0.007	1.164±0.016	1.166±0.018	0.310	1.143
AV	H ₂ O	B-3	1.326±0.014	[0.181±0.019]	-0.003	+0.042	1.184±0.023			
AV	H ₂ O	B-4	1.3348±0.0055	[0.224±0.019]	-0.003	+0.042	1.150±0.020			

* Corrected for effect of thimbles and foils

The results in Table 2 illustrate that although the two measurements of buckling for the air-cooled fuel assemblies were made in markedly different lattices (i.e. the AQ lattice D_2O -reflected, the AX lattice a three-region core) the two results are in good agreement with one another and also with earlier measurements⁽⁵⁾ made in triangular lattices using the same fuel assemblies. This confirms the validity of the one-group, constant cadmium ratio method used here.

Also listed in Table 2 are buckling values given by the lattice calculation codes LATREP and P000F. It is evident from the table that P000F agrees better with the absolute values of the experimental bucklings and also is in much better agreement with the buckling difference between the H_2O and air-cooled lattices, i.e. the void coefficient.

(c) Extrapolation Lengths

Extrapolation lengths were determined from the neutron activation distributions. For the air-cooled lattices the radial extrapolation length is defined as

$$\delta_R = R_{ex} - R_c = \frac{2.4048}{\lambda} - R_c \quad (7)$$

where R_c is the equivalent core radius defined for a square lattice by

$$R_c = 0.564 d \sqrt{N} \quad (8)$$

where d = lattice pitch

N = number of fuel assemblies

The total axial extrapolation length δz_t is defined as

$$\begin{aligned}\delta z_t &= H_{\text{ex}} - (H_{\text{D}_2\text{O}} - 15) \\ &= \frac{\pi}{\alpha} - (H_{\text{D}_2\text{O}} - 15) = \delta z_u + \delta z_l\end{aligned}$$

where $H_{\text{D}_2\text{O}} - 15$ is the distance in cm from the bottom of the fuel to the critical moderator level;

$$\delta z_u = \frac{H_{\text{ex}}}{2} - (H_{\text{D}_2\text{O}} - z_o) = \text{upper extrapolation length, and}$$

$$\delta z_l = \frac{H_{\text{ex}}}{2} - (z_o - 15) = \text{lower extrapolation length.}$$

Values of the extrapolation lengths are listed in Table 3. Errors quoted are derived from the errors in α , λ , z_o and $H_{\text{D}_2\text{O}}$.

2. Coolant Loss Experiments

(a) Activity Distributions

Fig. 12 to 17 show the copper foil relative activity distributions along the North-South and East-West directions for the various lattices.

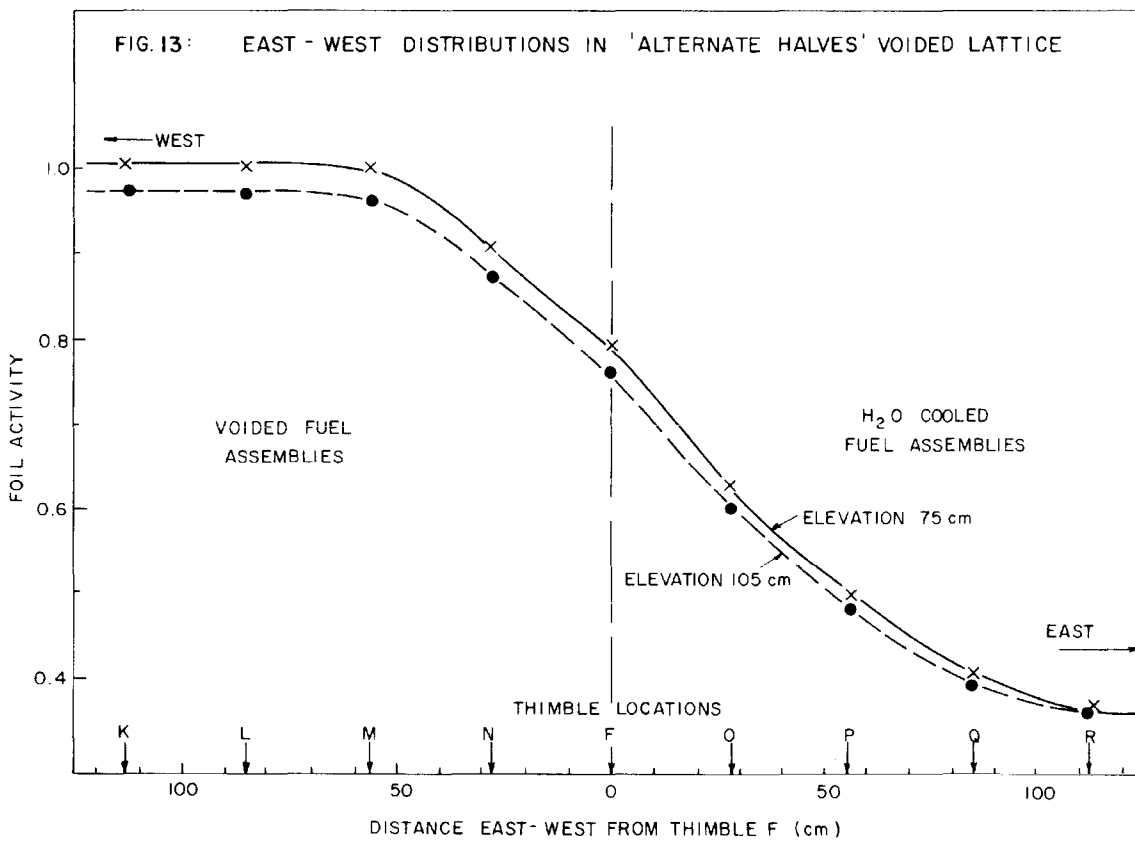
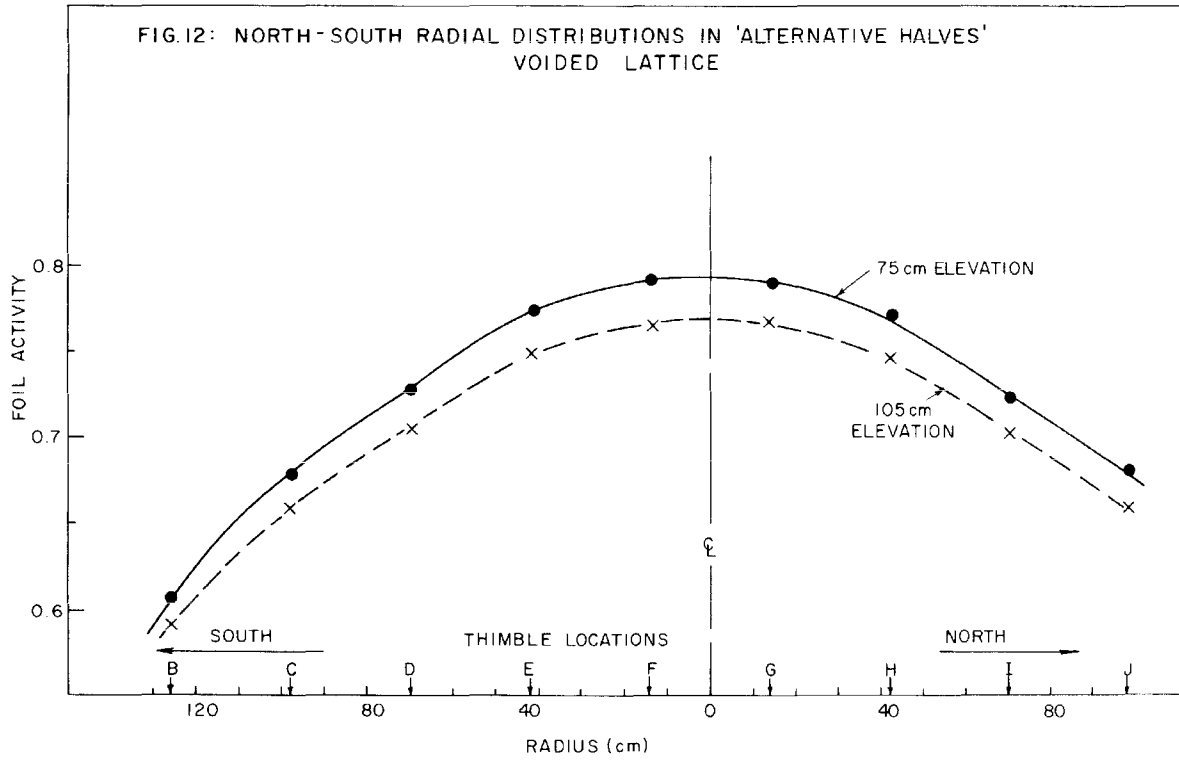
In the 'alternate halves' lattice (see Fig. 12 and 13) the North-South distribution is fairly symmetric as expected whilst the East-West distributions illustrate a steep profile across the lattice, the flux in the voided half being considerably higher (\sim a factor of two) than in the H_2O -cooled region.

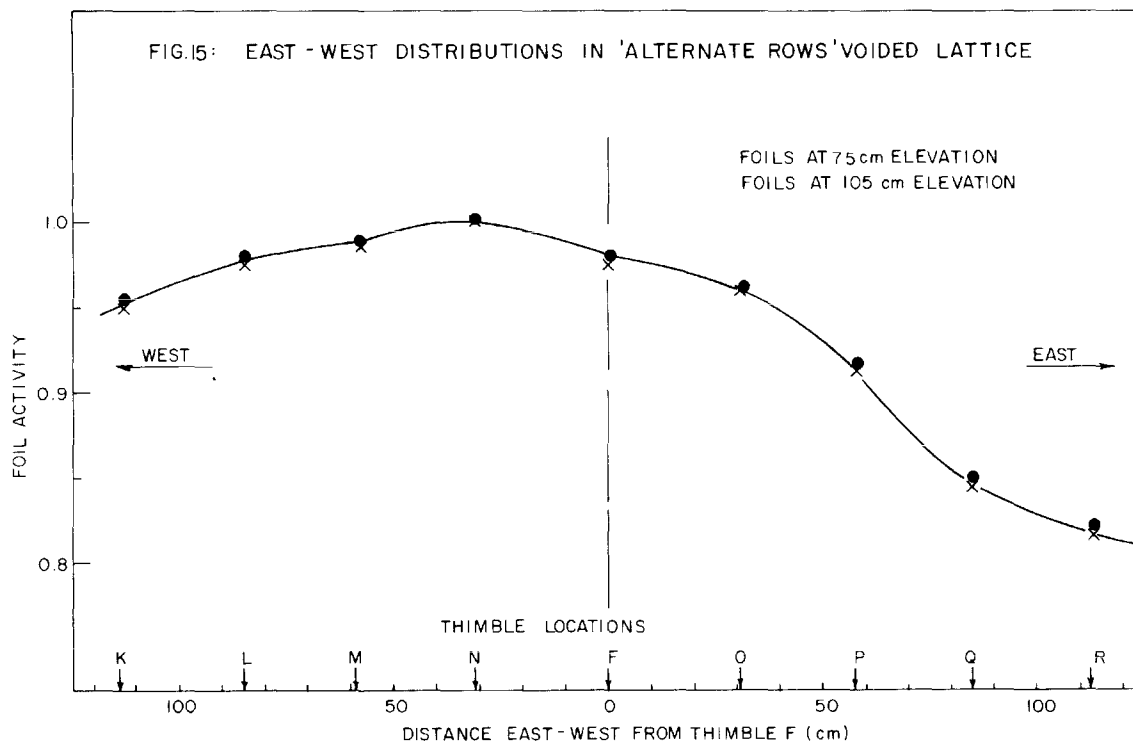
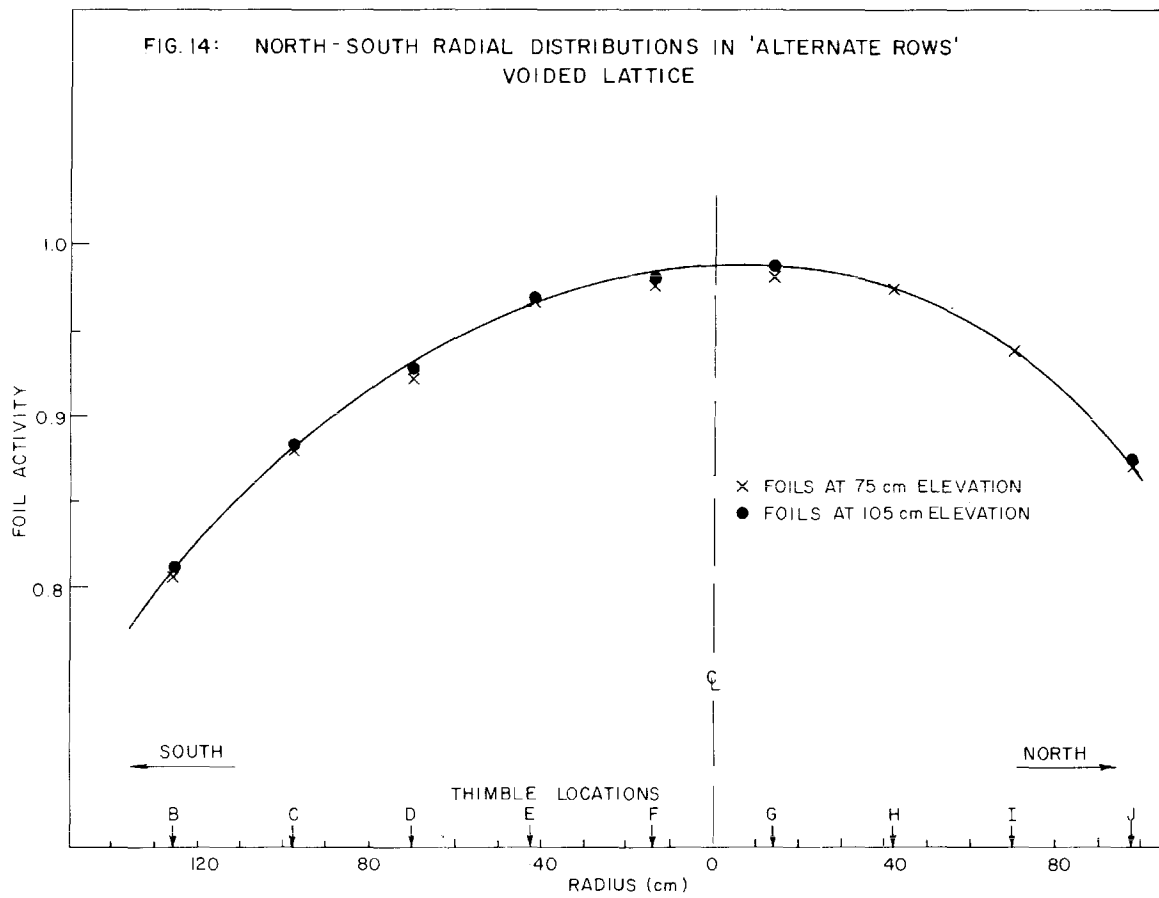
Fig. 14 to 17 illustrate that in the 'alternate row' and 'alternate assembly' lattices, the more homogeneous voidage leads as expected to more nearly symmetrical distributions across the lattice.

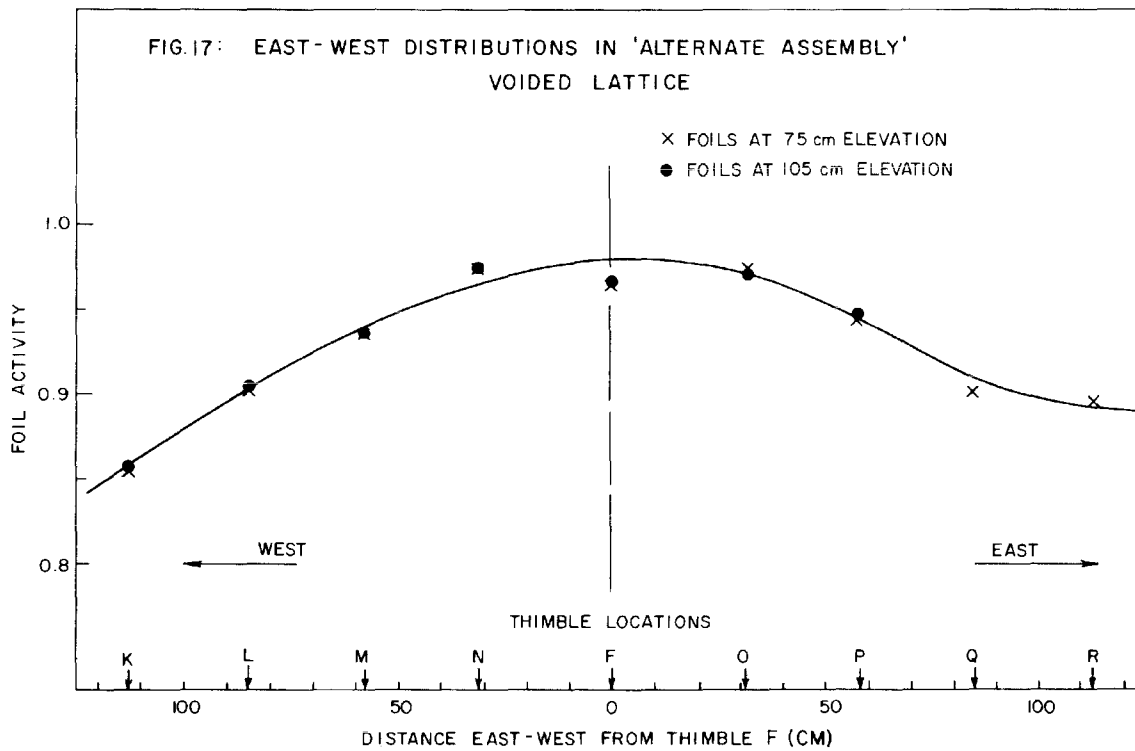
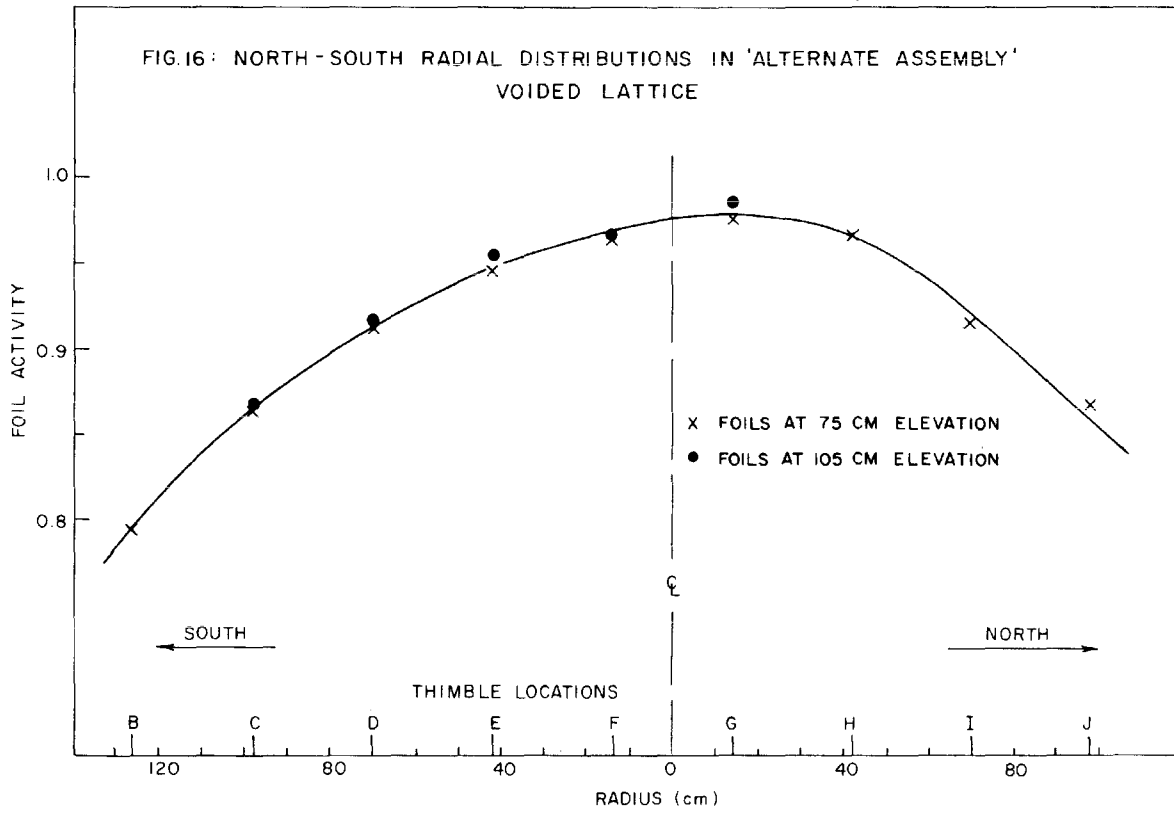
TABLE 3: SUMMARY OF EXTRAPOLATION LENGTHS IN 28 ROD UO_2 ,
AIR AND H_2O COOLED LATTICES

Lattice	Coolant	Table Number	R_{ex} cm	δR cm	H_{D_2O} cm	H_{ex} cm	z_o cm	δz_t cm	δz_u cm	δz_l cm
AQ	AIR	B-1	167.4 \pm 1.6	52.7 \pm 1.61	201.38	226.02 \pm 0.88	94.23 \pm 0.18	39.64 \pm 0.90	5.86 \pm 0.68	33.78 \pm 0.65
AX	AIR	B-5	258.6 \pm 6.7	144.9 \pm 6.7	156.40	181.4 \pm 1.3	74.36 \pm 0.43	40.0 \pm 1.3	8.7 \pm 1.0	31.33 \pm 0.99
AS	H_2O	B-2			244.19	265.21 \pm 0.77	117.97 \pm 0.17	36.02 \pm 0.79	6.38 \pm 0.61	29.64 \pm 0.58
AV	H_2O	B-3			251.27	274.1 \pm 1.4	120.32 \pm 0.24	37.9 \pm 1.4	6.1 \pm 1.4	31.7 \pm 1.3
AV	H_2O	B-4			250.83	272.76 \pm 0.57	120.13 \pm 0.23	36.92 \pm 0.60	5.68 \pm 0.50	31.25 \pm 0.46

NOTE: The above data are for the temperature and purity conditions of the experiments, with foils and thimbles present.







(b) Cadmium Ratios

The Cd ratios obtained using the bare and cadmium-covered In foil activities (corrected for height differences) in the 'alternate assembly' lattice are illustrated in Fig. 18. Values are given in Table A4. In the BLW region of the lattice at radii $< \sim 85$ cm the cadmium ratio is essentially constant. The East-West distribution shows an asymmetry at $r > \sim 75$ cm due to differences in the lattice near the BLW-buffer transition region.

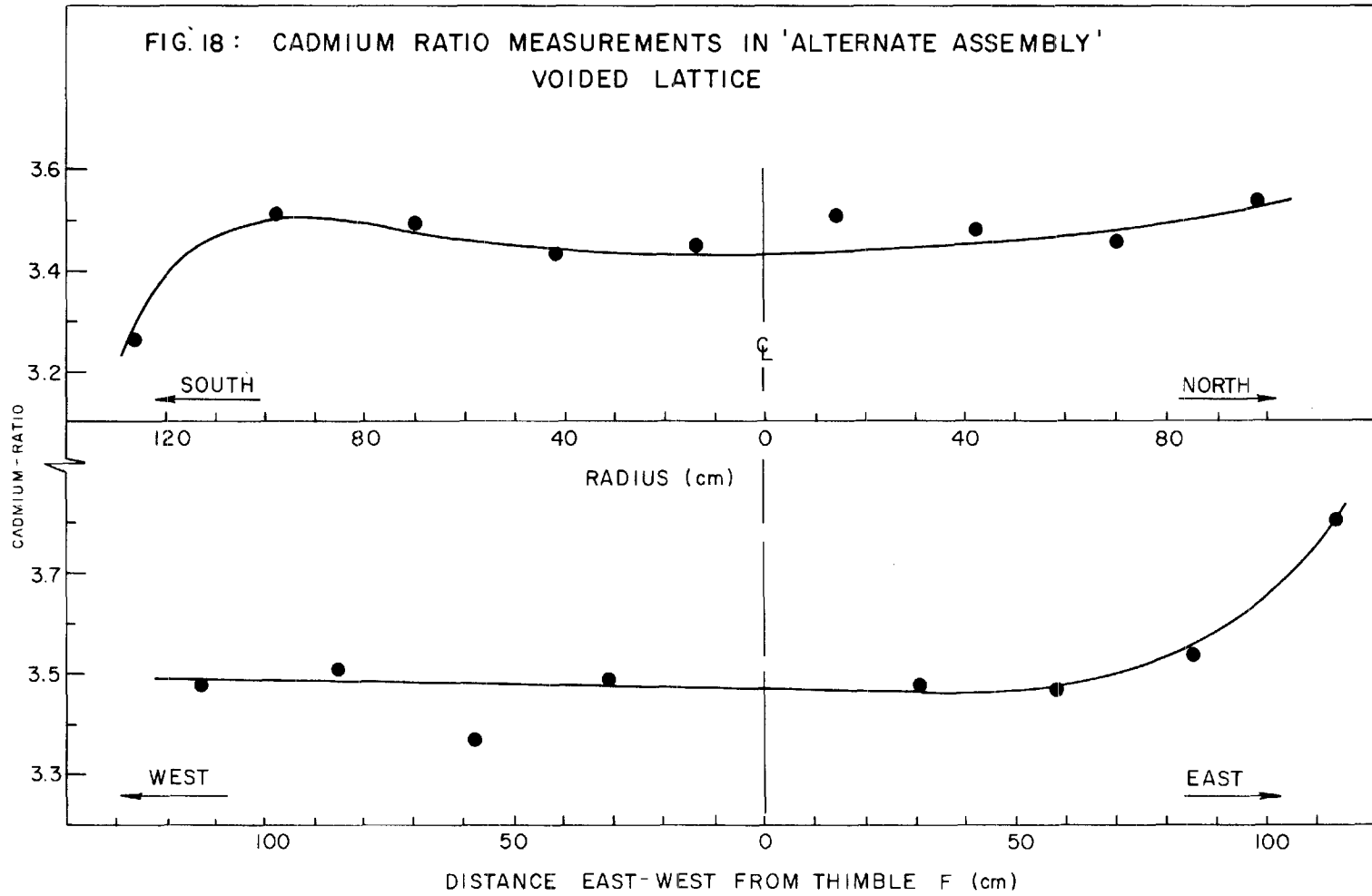
Cadmium ratios for a completely voided or fully H₂O-cooled BLW lattice are shown in Fig. 9 to 11. These should correspond to the values in the two halves of the 'alternate halves' lattice well-removed from the boundaries. The Cd ratios for the various core conditions are listed in Table 4 along with the corresponding Westcott $r \sqrt{\frac{T}{T_0}}$ values derived using the method described by Bigham et al.⁽⁹⁾

Table 4: Cd Ratios and $r \sqrt{\frac{T}{T_0}}$ Values

Core Type	Cd Ratio	$r \sqrt{\frac{T}{T_0}}$
All assemblies H ₂ O-cooled:	3.945	0.0214
All assemblies air-cooled:	3.091 ^a 3.070 ^b	0.0305 ^a 0.0308 ^b
Alternate assemblies voided:	3.472	0.0257

^aLattice AX (driven) ^bLattice AQ (undriven)

FIG. 18 : CADMIUM RATIO MEASUREMENTS IN 'ALTERNATE ASSEMBLY'
VOIDED LATTICE



(c) Reactivity Measurements

The results of the critical height measurements with the different arrangements of coolant voids are given in Table 5. The results have been expressed as reactivity values, δk_{eff} , using the relationship,

$$\delta k_{\text{eff}}(x) = \frac{M_{\text{eff}}^2(x) B^2(x) - M_{\text{eff}}^2(\text{H}_2\text{O}) B^2(\text{H}_2\text{O})}{1 + M_{\text{eff}}^2(\text{H}_2\text{O}) B^2(\text{H}_2\text{O})} \quad (9)$$

where x signifies a particular voided configuration,

H_2O the fully H_2O -cooled lattice, and

$$M_{\text{eff}}^2 = L^2 + L_s^2 + L^2 L_s^2 B^2 \quad (10)$$

where L^2 and L_s^2 are the thermal diffusion and slowing down areas respectively obtained from the POOF code.

For the partial void cases the values of radial buckling, L^2 and L_s^2 used were the average of those for the fully voided and fully H_2O -cooled lattices, i.e. AX and AV. The values of L^2 and L_s^2 used were for moderator conditions of 22°C and 99.66 atom % D_2O . No allowance has been made for the fact that the various lattices did not have the same temperature and moderator purity since the effects are small (< 1%) compared to the accuracy of the rather simple model used here.

Although the method may not be rigorous it does serve to show that there is a significantly larger ($\sim 11\%$) reactivity effect when half the coolant is voided on one side of the lattice than when alternate rows or alternate assemblies are voided, the latter two cases giving essentially the same reactivity change. This enhanced reactivity effect for the alternate halves arrangement was predicted by calculations done by Kerr and Primeau. (10)

TABLE 5. REACTIVITY EFFECTS OF COOLANT LOSS

Lattice	Date	H _{D₂O}	D ₂ O Temp.	D ₂ O Purity	H _{ex}	α ²	λ ² , [ν ²]	B ²	M _{eff} ²	δk _{eff}
		cm	°C	a/o	cm	m ⁻²	m ⁻²	m ⁻²	cm ²	milli-k
AV (H ₂ O-cooled)	19/10/66	250.00	22.05	99.662	271.95	1.335	[0.202]	1.132	284.54	-
Alternate Halves (50% Void)	1/11/66	177.83	21.77	99.661	201.21	2.438	0.332*	2.770	318.18	54.2
Alternate Rows (50% Void)	2/11/66	187.39	21.77	99.661	210.77	2.222	0.332*	2.554	317.66	47.4
Alternate Assemblies (50% Void)	4/11/66	186.84	22.36	99.660	210.22	2.233	0.332*	2.565	317.69	47.7
AX (100% Void)	8/11/66	155.94	21.80	99.659	180.94	3.015	0.865	3.880	351.93	101.1
AQ (100% Void)	20/6/66	200.74	21.94	99.718	225.38	1.943	2.063	4.006	352.29	105.5

* Taken as average of lattice AX and AV values.

The fact that the two rather different air-cooled lattices gave reactivity values in good agreement with each other gives some confidence in the method.

CONCLUSIONS

Bucklings have been obtained for 28-rod natural uranium oxide fuel assemblies in a 27.94 cm square lattice with air and H₂O as coolants. As expected, the air-cooled lattice yielded a much higher buckling value than the H₂O-cooled lattice due to the absorption by the H₂O. The measured buckling difference should provide a good check on the lattice codes used to calculate the void coefficient for the CANDU-BLW reactor.

Measurements of buckling made in the multiregion air-cooled lattice were in good agreement with the value obtained in a normal heavy water-reflected lattice, illustrating the applicability of the one-group, constant cadmium ratio technique for these measurements.

Experiments were also performed to investigate the reactivity effects of voiding 50% of the fuel assemblies. Three geometric arrangements of voidage were investigated. The largest increase in reactivity was produced by voiding half the fuel assemblies about a diameter. Smaller (by ~ 11%) reactivity effects were produced for lattices where alternate rows of fuel assemblies or alternate fuel assemblies were voided. Essentially no difference was observed between the latter two cases, suggesting that no further subdivision beyond the alternate rows arrangement is necessary for the dual circuit primary coolant system of the BLW reactor.

ACKNOWLEDGEMENTS

The authors wish to thank all those who contributed during the course of this work. In particular we acknowledge the assistance of D.H. Walker who was responsible for the overall operation of the reactor and P.D.J. Ferrigan, E.J. Pleau and D.J. Roberts who helped with the experiments. J.T.R. Young was responsible for the foil counting and also prepared some of the drawings. Mrs. A. Brum and Miss D. Graham ran various computer programs and Mrs. S. Argue and Mrs. N.G. Hulbert typed manuscripts.

We also acknowledge the helpful comments of Dr. C.H. Millar concerning the presentation of the report.

REFERENCES

- (1) R.E. Kay, C.J. Tanner; CANDU-BLW Experiments in ZED-2. Part I: Refuelling Experiment; AECL-2667 (1967).
- (2) R.E. Kay; CANDU-BLW Experiments in ZED-2. Part II: Booster Rod Experiments; AECL-2689 (1967).
- (3) G.A. Pon, G.R. Boucher; Gentilly Nuclear Power Station; Paper Presented at the Eleventh AECL Symposium on Atomic Power; AECL-2486 (1966).
- (4) ZED-2; IAEA Directory of Nuclear Reactors, 5, 223 (1964).
- (5) K.J. Serdula; Lattice Measurements with 28-Element Natural UO_2 Fuel Assemblies. Part I: Bucklings for a Range of Spacings with Three Coolants; AECL-2606 (1966).
- (6) G.A. Beer, D.W. Hone; Lattice Measurements with 7-Element UO_2 Clusters in ZED-2. Part I: Bucklings Over a Range of Spacings with Three Coolants; AECL-1505 (1962).
- (7) D.W. Hone et al.; Natural Uranium Heavy Water Lattices, Experiment and Theory; Proceedings of Second Geneva Conference on the Peaceful Uses of Atomic Energy, 12, 351 (1958).
- (8) M.F. Duret, R. Marriott; A Computer Program for Reactor Studies; AECL-911 (1959).
- (9) C.B. Bigham et al.; Experimental Effective Fission Cross Sections and Neutron Spectra in a Uranium Fuel Rod. Part II: CANDU-Type Uranium Oxide Clusters; AECL-1350 (1961).
- (10) R.E. Kerr, D.B. Primeau; Private Communication (1966).

APPENDIX A

RESULTS OF CADMIUM RATIO

MEASUREMENTS

TABLE A-1: CADMIUM-RATIO MEASUREMENTS

AQ LATTICE, 27.94cm (11") SQ. AIR COOLED

June 21st 1966		H _{D20} = 199.487cm				Temp. = 22.09°C			
Thimble	K7W	K5W	K3W	K1W	K1E	K3E	K5E	K7E	
Radius (cm)	97.79	69.85	41.91	13.97	13.97	41.91	69.85	97.79	
Elevation 75cm.	3.396	3.049	3.045	3.078	3.062	3.128	3.055	3.384	

TABLE A-2: CADMIUM-RATIO MEASUREMENTS BLW(AS) LATTICE, 27.94cm (11") SQ., H₂O COOLED

July 22nd 1966		H _{D20} = 244.343cm				Temp. = 22.25°C					
Thimble	K9W	K7W	K5W	K3W	K1W	K1E	K3E	K5E	K7E	K9E	Z
Radius (cm)	125.73	97.79	69.85	41.91	13.97	13.97	41.91	69.85	97.79	125.73	149.97
Elevation 125cm.	3.608	3.946	3.981	3.971	2.915*	3.906	3.943	3.926	3.555	3.754	2.766

*Flyer

TABLE A-3: CADMIUM-RATIO MEASUREMENTS

AX LATTICE 27.94cm (11") SQ, AIR COOLED

November 10th 1966		$H_{D20} = 156.956\text{cm}$								Temp. = 22.14°C
Thimble	B0	C0	D0	E0	F0	G0	H0	I0	J0	
Radius (cm)	125.73	97.79	69.85	41.91	13.97	13.97	41.91	69.85	97.79	
Elevation 55cm.	2.891	3.125	3.085	3.104	3.082	3.068	3.156	3.104	3.250	
Thimble	F8W	F6W	F4W	F2W	F2E	F4E	F6E	F8E		
Radius (cm)	112.63	84.98	57.60	31.24	31.24	57.60	84.98	112.63		
Elevation 55cm.	3.395	3.108	3.078	3.091	3.086	3.056	3.126	3.402		

TABLE A-4: CADMIUM-RATIO MEASUREMENTS

AW LATTICE ALTERNATE ASSEMBLIES VOIDED

November 4th 1966		$H_{D20} = 188.037\text{cm}$								Temp. = 22.0°C
Thimble	B	C	D	E	F	G	H	I	J	
Radius (cm)	125.73	97.79	69.85	41.91	13.97	13.97	41.91	69.85	97.79	
Elevation 75 cm.	3.268	3.513	3.486	3.427	3.447	3.505	3.476	3.464	3.542	
Thimble	K	L	M	N	O	P	Q	R		
Radius (cm)	112.63	84.98	57.60	31.24	31.24	57.60	84.98	112.63		
Elevation 75 cm.	3.483	3.511	3.371	3.493	3.476	3.466	3.539	3.810		

APPENDIX B

BUCKLING DATA

TABLE B-1: BUCKLING DATA - LATTICE AQL, 27.94cm (11") SQ, AIR COOLED

		<u>Moderator</u>						
June 20th 1966	Manganese-Nickel Foils	Temp : 21.94°C Purity : 99.718 atom % D ₂ O					H _{D2O} = 201.384cm	
Direction	W	W	W	W	E	E	E	E
Thimble	K7	K5	K3	K1	K1	K3	K5	K7
Radius (cm)	97.79	69.85	41.91	13.97	13.97	41.91	69.85	97.79
Elevation (cm)								
195				(.1422)	(.1423)			
185				(.2926)	(.2916)			
175				(.4301)	(.4365)			
165				.5583	.5523			
155				.6637	.6586			
145				.7582	.7523			
135				.8430	.8360			
125				.9136	.9020			
115				.9678	.9573			
105	(.5852)	.7544	.9060	.9940	.9799	.9096	.7645	(.5753)
95	(.9517)	.7625	.9140	1.0000	.9868	.9116	.7702	(.5780)
85	(.5856)	.7565	.9076	.9898	.9752	.9071	.7628	(.5738)
75				.9679	.9547			
65				.9313	.9149			
55				.8605	.8506			
45				.7759	.7600			
35				(.6823)	(.6716)			
25				(.5911)	(.5802)			
15				(.5180)	(.5123)			

<u>J₀ Fits</u>				<u>Cosine Fits</u>		
Elevation (cm)	105	95	85	Thimble	K1W	K1E
Number of Points	3	3	3	Number of points	13	13
East Fit λ(m ⁻¹)	1.409	1.406	1.403	z ₀ (cm)	94.06	94.41
West Fit λ(m ⁻¹)	1.476	1.465	1.460	α (m ⁻¹)	1.3895	1.3904
Average λ(m ⁻¹)	1.436 ± 0.014			Bare Lattice α (m ⁻¹)	1.3939 ± 0.0054	

TABLE B-2: BUCKLING DATA - LATTICE AS, 27.94cm (11") SQ, H₂O COOLANT

July 21st 1966	Manganese-Nickel Foils					Temp: 22.58°C					Purity: 99.707 atom % D ₂ O					H ₂ O = 244.194cm	
Direction	W	W	W	W	W	E	E	E	E	E	SW	SW	SW	NE	NE	NE	N
Thimble	K9	K7	K5	K3	K1	K1	K3	K5	K7	K9	J1	J3	I5	L1	L3	M5	Z
Radius (cm)	125.73	97.79	69.85	41.91	13.97	13.97	41.91	69.85	97.79	125.73	31.24	50.37	89.46	31.24	50.37	89.46	149.97
Elevation (cm)																	
235						(1745)											(1307)
225						(3020)											(2222)
215						4196											3057
205						5275											3808
195						6256											4503
185						7178											5148
175						8028											5725
165						8782											6203
155						9348											6624
145	(9547)	(10520)	10120	9870	9762	9730	9905	10078	(10339)	(9515)	9881	9836	10277	9833	9851	10158	6915
135	(9873)	(10855)	10418	10182	10110	10000	10249	10408	(10633)	(9804)	10184	10173	10603	10086	10219	10486	7138
125	(10085)	(10969)	10639	10379	10313	10219	10464	10606	(10898)	(10005)	10436	10397	10817	10332	10420	10696	7262
115						10348											7276
105						10153											7226
95						9864											7061
85						9439											6779
75						8925											6422
65						8359											5984
55						7570											5466
45						6672											4870
35						(5751)											(4233)
25						(4842)											(3613)
15						(4109)											(3258)

I₀ Fits

Elevation (cm)	145	135	125
No. of Points	3	3	3
East Fit, ν (m ⁻¹)	0.5406	0.5837	0.5483
West Fit, ν (m ⁻¹)	0.5585	0.5139	0.5244
Northeast Fit, ν (m ⁻¹)	0.4447	0.4646	0.4446
Southwest Fit, ν (m ⁻¹)	0.5027	0.5025	0.4791
Average ν (m ⁻¹)	0.5089 ± 0.0129		

Cosine Fits

Thimble	K1E	Z
No. of points	18	18
z ₀ (cm)	117.97	117.28
α (m ⁻¹)	1.1846	1.1640
Bare lattice α (m ⁻¹)	1.1880 ± 0.0035	

TABLE B-3: BUCKLING DATA - LATTICE AV, 27.94cm (11") SQ, H₂O COOLANT

October 19th 1966 (a.m.)	Manganese-Nickel Foils								Temp: 22.05°C	Purity: 99.660 atom % D ₂ O				H _{D₂O} = 251.269cm			
Direction	S	S	S	S	S	N	N	N	N	W	W	W	W	E	E	E	E
Thimble	B0	C0	D0	E0	F0	G0	H0	I0	J0	F8	F6	F4	F2	F2	F4	F6	F8
Radius (cm)	125.73	97.79	69.85	41.91	13.97	13.97	41.91	69.85	97.79	112.63	84.98	57.60	31.24	31.24	57.60	84.98	112.63
Elevation (cm)																	
235						(2431)	(2523)										
225						(3568)	(3674)										
215						4659	4764										
205						5635	5734										
195						6525	6607										
185						7340	7398										
175						8053	8126										
165						8717	8777										
155						9184	9252										
145						9560	9599										
135	(9872)	(10451)	10078	9969	9844	9833	9909	10034	(10244)	(10670)	10293	10036	9881	9876	10117	10099	(10766)
125	(10024)	(10592)	10222	10122	10000	10064	10066	10181	(10396)	(10845)	10418	10182	10045	10055	10259	10245	(10922)
115					10100	10104											
105	(9924)	(10455)	10088	9993	9887	9939	9928	10021	(10311)	(10781)	10253	10048	9878	9861	10177	10096	(10806)
95					9587	9621											
85					9196	9203											
75					8690	8740											
65					8067	8161											
55					7326	7343											
45					6428	6462											
35					(5557)	(5570)											
25					(4664)	(4687)											
15					(3943)	(3918)											

<u>I₀ Fits</u>			
Elevation (cm)	135	125	105
No. of Points	6	6	6
North+East Fit, ν (m ⁻¹)	0.3954	0.3569	0.3820
South+West Fit, ν (m ⁻¹)	0.4880	0.4746	0.4561
Average ν (m ⁻¹)	0.4255 ± 0.0222		

<u>Cosine Fits</u>		
Thimble	FOS	GON
No. of Points	18	18
z ₀ (cm)	120.27	120.37
α (m ⁻¹)	1.1518	1.1401
Bare Lattice α (m ⁻¹)	1.1514 ± 0.0059	

TABLE B-4: BUCKLING DATA - LATTICE AV, 27.94cm (11") SQ, H₂O COOLANT

October 19th 1966 (p.m.)	Manganese-Nickel Foils						Temp: 22.14°C	Purity: 99.660 atom % D ₂ O	HD ₂ O = 250.833cm			
Direction	W	W	W	W	W	S	N	E	E	E	E	E
Thimble	D6	D4	E4	E2	F2	F0	G0	G2	H2	H4	I4	I6
Radius (cm)	109.11	89.45	69.85	50.37	31.24	13.97	13.97	31.24	50.37	69.85	89.45	109.11
Elevation (cm)												
235						(2389)	(2439)					
225						(3524)	(3581)					
215						4621	4671					
205						5583	5648					
195						6469	6518					
185						7281	7283					
175						8029	8005					
165						8687	8663					
155						9154	9147					
145						9548	9521					
135	10899	10267	10051	9884	9796	9790	9792	9808	9776	10022	10163	10891
125	11033	10440	10194	10030	9960	10000	9952	9959	9909	10237	10300	10997
115						10055	9989					
105	10872	10312	10062	9929	9821	9907	9875	9801	9743	10138	10187	10906
95						9605	9554					
85						9063	9176					
75						8666	8640					
65						8038	8044					
55						7268	7313					
45						6448	6467					
35						(5564)	(5544)					
25						(4672)	(4675)					
15						(3930)	(3876)					

<u>I₀ Fits</u>			
Elevation (cm)	135	125	105
No. of Points	5	5	5
Southwest Fit, $\nu(m^{-1})$	0.5033	0.4748	0.4818
Northeast Fit, $\nu(m^{-1})$	0.4577	0.4627	0.4604
Average $\nu(m^{-1})$	0.4734 \pm 0.0070		

<u>Cosine Fits</u>		
Thimble	FOS	GON
No. of Points	18	18
z_0 (cm)	120.18	120.08
$\alpha(m^{-1})$	1.1539	1.1497
Bare Lattice $\alpha(m^{-1})$	1.1554 \pm 0.0024	

TABLE B-5: BUCKLING DATA - LATTICE AX, 27.94cm (11") SQ, AIR COOLANT

November 8th 1966	Manganese-Nickel Foils								Temp: 21.83°C	Purity: 99.659 atom % D ₂ O				H _{D2O} = 156.398cm			
Direction	S	S	S	S	S	N	N	N	N	W	W	W	W	E	E	E	E
Thimble	B0	C0	D0	E0	F0	G0	H0	I0	J0	F8	F6	F4	F2	F2	F4	F6	F8
Radius (cm)	125.73	97.79	69.85	41.91	13.97	13.97	41.91	69.85	97.79	112.63	84.98	57.60	31.24	31.24	57.60	84.98	112.63
Elevation (cm)																	
155					(955)	(1046)											
145					(3038)	(3148)											
135					(4756)	(4881)											
125					6259	6397											
115					7560	7704											
105					8493	8677											
95					9162	9350											
85					9663	9850											
75	(7175)	(7958)	8855	9535	9861	10000	9678	8951	(8018)	(7966)	8568	9206	9779	9689	9288	8414	(7897)
65					9803	9951											
55	(6780)	(7519)	8375	9015	9345	9460	9172	8436	(7541)	(7524)	8062	8730	9216	9142	8778	7950	(7453)
45					8578	8710											
35					(7684)	(7801)											
25					(6780)	(6884)											
15					(6098)	(6131)											

J₀ Fits

Elevation (cm)	75	55
No. of Points	6	6
South+West Fit, $\lambda(m^{-1})$	0.9018	0.9118
North+East Fit, $\lambda(m^{-1})$	0.9541	0.9528
Average $\lambda(m^{-1})$	0.930 ± 0.024	

Cosine Fits

Thimble	F0S	G0N
No. of Points	9	9
z ₀ (cm)	74.18	74.54
$\alpha(m^{-1})$	1.7332	1.7350
Bare Lattice $\alpha(m^{-1})$	1.736 ± 0.012	